2026 IEEE International Conference on Robotics and Automation (ICRA 2026)
June 1-5, 2026. Vienna, Austria

Throw Maneuver: Exact Trajectories for Invariant Target Hitting in Robotic Throwing

Sheng Cheng*, Ziyin Han*, Rong Wang, Naira Hovakimyan

***Abstract*— Robots can throw objects to distant targets using gravity, with applications ranging from material transport to firefighting. Existing approaches typically adopt a singleton throw formulation, where the carrier must reach a specific position–velocity configuration at the moment of throw. This reliance on a single throw point makes target-hitting highly sensitive to release delays. To address this limitation, we introduce the throw maneuver: a carrier trajectory that guarantees target hitting for objects released at any time along the trajectory. By differentiating the governing projectile equations, we derive the throw maneuver in its exact representation as ordinary differential equations, with analytical solutions available in special cases. Simulation results verify its invariant target-hit property and show that throw maneuvers achieve longer available throw time and ranges without target miss compared with a strong baseline throw method. Outdoor quadrotor experiments further demonstrate throw maneuver's improved accuracy and precision under realistic flight conditions compared with several baseline throw methods.**

***Index Terms*— Robotic throwing, trajectory planning, aerial robotics.**

I. INTRODUCTION

Throwing is a dynamic robotic skill that exploits gravity to deliver an object to a target that is otherwise out of reach. This makes robotic throwing an attractive capability for applications ranging from material transport to firefighting.

The simplest way to realize a robotic throw is to drive the carrier to a specific position with a particular velocity, and then trigger the release at that moment. The required position–velocity configuration can be precomputed from the target's location, which, however, usually forms only a single point in the configuration space, yielding a singleton throw set. Much of the existing literature has focused on this singleton formulation, where planning methods [1]–[5] have sought to generate appropriate trajectories to reach this point, and control strategies [5]–[9] have been developed to execute them robustly and accurately.

A major limitation of the singleton throw is that the release must occur at a specific point in space and time. In practice, inevitable delays between issuing the command and executing the release often cause the carrier to miss this point, resulting in a failed throw. To mitigate this sensitivity, researchers have investigated formulations that yield a continuum of throw points beyond the single point. Early work [10] addresses this problem through a two-point boundary value problem, solving for manipulator control that achieve the desired goal state of the thrown object. More recently, the notion of tube acceleration has been introduced [11], which uses an optimization problem to solve for a constant-acceleration joint motion within feasible manipulator configurations. The authors apply convex relaxation to the problem and solve for the constant acceleration. This relaxation, justified under the assumption of a short throw window, applies a first-order approximation to the nonlinear equality constraint on the projectile motion that governs the end-effector's position and velocity for target hit. The tube acceleration has since been applied to a legged mobile manipulator to achieve reliable throwing under motion uncertainties [12]. However, the first-order approximation yields target miss when release delays exist, and the short-throw-window assumption limits the permissible time and range to perform the throw, further limiting the applications of tube acceleration.

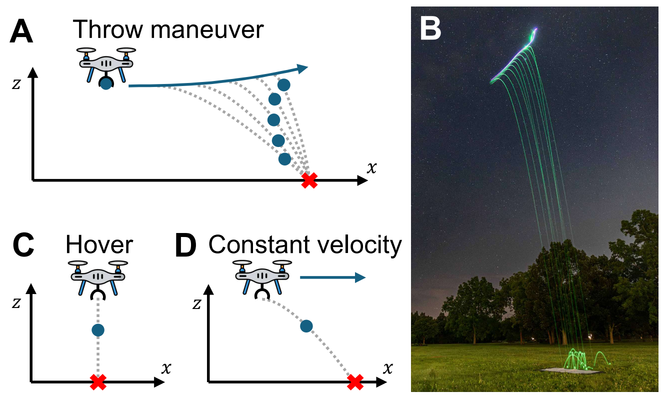

Fig. 1: Illustration of throw methods. A: Proposed throw maneuver. B: Long exposure of a quadrotor carrier sequentially throwing multiple golf balls to hit a target on the ground. C: Conventional hover throw. D: Conventional constant-velocity throw.

In line of a continuum of throw points, we characterize a class of trajectories along which an object can reach the target if released *at any moment*. We refer to such a trajectory as the *throw maneuver*. This trajectory's exact representation is a set of ordinary differential equations (ODEs) derived by differentiating the governing projectile equations with respect to throw time. In certain cases, the trajectory admits an analytical solution, making it particularly useful for applications such as quadrotor-based throwing. We validate in simulation that, when following a throw maneuver, objects consistently reach the target regardless of throw time, which yields robust throwing subject to release delays. We further

This work is supported by NASA ULI (80NSSC22M0070), NSF SLES (2331878), NSF M3X (2431216), and AFOSR DURIP (FA9550-23-1-0129).

Authors are with the Department of Mechanical Science and Engineering, University of Illinois Urbana-Champaign, USA. Email: {chengs, ziyinh2, rongw5, nhovakim}@illinois.edu
*These authors contribute equally to this work.

demonstrate the approach in outdoor quadrotor experiments under realistic flight conditions, evaluating both accuracy and precision of objects' landing points. The results show that throw maneuvers significantly outperform kinetic baseline methods such as constant-velocity and tube-acceleration throws [11], achieving more reliable target hits in practice.

The contributions of this paper are summarized as follows: We present an exact characterization of a carrier trajectory such that an object released from the carrier will reach the target regardless of the throw time. Unlike prior work that relies on relaxation or approximation [11], [12], our derivation is exact and admits analytical solutions in certain cases. This formulation enables robust throwing in the presence of release delays and further supports sequential throwing of multiple objects with theoretical guarantees of reaching the target. Together, these results establish a new paradigm for robotic throwing applications.

II. Background

We begin with the basics of throw. Suppose a carrier throws an object to hit a target on the ground. It suffices to consider the carrier's motion in a vertical 2D plane shown in Fig. 1, as the object's projectile remains within this plane once thrown by the carrier. We define a 2D coordinate system with a horizontal axis x and a vertical axis z. Without loss of generalization, we set the target at the origin for convenience. We assume the object undergoes a free fall without aerodynamic drag. Denote the carrier's position and velocity by $\boldsymbol{p} = \left[\begin{smallmatrix}\boldsymbol{p}_x \\ \boldsymbol{p}_z\end{smallmatrix}\right]$ and $\boldsymbol{v} = \left[\begin{smallmatrix}\boldsymbol{v}_x \\ \boldsymbol{v}_z\end{smallmatrix}\right]$, respectively. When the carrier throws the object at height $\boldsymbol{p}_z$ and vertical velocity $\boldsymbol{v}_z$, the object's landing time T satisfies

$$\boldsymbol{p}_z + \boldsymbol{v}_z T - \frac{1}{2} g T^2 = 0. \tag{1}$$

The landing time allows to characterize the relationship between the carrier's horizontal position $\boldsymbol{p}_x$ and velocity $\boldsymbol{v}_x$ upon throwing the object, i.e.,

$$\boldsymbol{p}_x + \boldsymbol{v}_x T = 0. \tag{2}$$

We formally define the set of position-velocity configurations that satisfy (1) and (2) as the throw set $\mathcal{G}$:

$$\mathcal{G} = \{(\boldsymbol{p}, \boldsymbol{v}) | \text{(1) and (2) are satisfied.}\} \tag{3}$$

For the object to hit the target at the origin, the carrier shall throw the object precisely at the time when it reaches $(\boldsymbol{p}, \boldsymbol{v}) \in \mathcal{G}$. This stringent requirement of releasing at a single point in space and time makes the throwing task prone to failure from mechanical uncertainties, such as release delays.

III. Throw Maneuver

We look for a trajectory of the carrier, described by $(\boldsymbol{p}(t), \boldsymbol{v}(t))$ for $t \geq 0$, such that the *invariant target-hit property* holds, i.e., the object can hit the target if it is thrown *at any moment* from the carrier. Since the object thrown from the carrier at time t has the initial state $\boldsymbol{p}(t)$ and $\boldsymbol{v}(t)$, in order for the object to hit the target, the following two equations hold for all t:

$$\boldsymbol{p}_z(t) + \boldsymbol{v}_z(t) T(t) - \frac{1}{2} g T(t)^2 = 0, \tag{4}$$

$$\boldsymbol{p}_x(t) + \boldsymbol{v}_x(t) T(t) = 0. \tag{5}$$

Note that the landing time T is dependent on the time of throw t, i.e.,

$$T(t) = \frac{\boldsymbol{v}_z(t) + \sqrt{\boldsymbol{v}_z^2(t) + 2g\boldsymbol{p}_z(t)}}{g}. \tag{6}$$

Definition 1: The **throw maneuver** is a trajectory $\{(\boldsymbol{p}(t), \boldsymbol{v}(t)) | t \geq 0\}$ that satisfies (4) and (5).

By Definition 1, the throw maneuver is robust to release delays because every single point on the trajectory yields target hit, completely independent to the actual time of throw due to the release delays.

Remark 1: A trivial throw maneuver is $\boldsymbol{p}_x(t) = \boldsymbol{v}_x(t) = 0,\ \boldsymbol{p}_z(t) > 0$, i.e., the carrier stays on top of the target with arbitrary vertical motion. This includes the intuitive case where the carrier hovers on top of the target.

To derive a non-trivial throw maneuver, we differentiate (4) and (5) with respect to the time argument t and equate the derivative to 0, which leads to the governing equations of the carrier's motion as below:

$$0 = \boldsymbol{v}_z(t) + \dot{\boldsymbol{v}}_z(t) T(t) + \boldsymbol{v}_z(t) \dot{T}(t) - g T(t) \dot{T}(t), \tag{7}$$

$$\dot{\boldsymbol{v}}_x(t) = -\frac{1 + \dot{T}(t)}{T(t)} \boldsymbol{v}_x(t). \tag{8}$$

Remark 2: Any trajectory that satisfies the system of ODEs (7), (8) and kinematics

$$\dot{\boldsymbol{p}}_x(t) = \boldsymbol{v}_x(t), \quad \dot{\boldsymbol{p}}_z(t) = \boldsymbol{v}_z(t), \tag{9}$$

with an initial condition $(\boldsymbol{p}(0), \boldsymbol{v}(0)) \in \mathcal{G}$ is a throw maneuver.

One can observe from (8) that the carrier's horizontal motion is determined by T and $\dot{T}$. The landing time T is determined by the vertical motion following (7). Hence, one can obtain a throw maneuver either by determining the vertical motion first and then obtain the resulting landing time, or by specifying the landing time first and then determining the vertical motion. We will discuss each case in the following subsections. For simplicity, the time argument t will be omitted below when it does not affect clarity.

A. Throw maneuver with predefined vertical motion

In this case, one starts with defining the vertical motion governed by $(\boldsymbol{p}_z, \boldsymbol{v}_z, \dot{\boldsymbol{v}}_z)$. Consequently, the landing time is determined by (7), rewritten in the following form:

$$\dot{T} = \frac{1}{g} \left(\dot{\boldsymbol{v}}_z + \frac{\boldsymbol{v}_z \dot{\boldsymbol{v}}_z + g \boldsymbol{v}_z}{\sqrt{\boldsymbol{v}_z^2 + 2g\boldsymbol{p}_z}} \right), \tag{10}$$

with initial condition $T(0)$ given by (6) at $t = 0$.

The horizontal motion follows as

$$\frac{\mathrm{d}}{\mathrm{d}t} \begin{bmatrix} \boldsymbol{p}_x \\ \boldsymbol{v}_x \end{bmatrix} = \begin{bmatrix} 0 & 1 \\ 0 & -\frac{1+\dot{T}}{T} \end{bmatrix} \begin{bmatrix} \boldsymbol{p}_x \\ \boldsymbol{v}_x \end{bmatrix}, \tag{11}$$

with initial condition satisfying $\boldsymbol{p}_x(0) = -\boldsymbol{v}_x(0) T(0)$.

Remark 3: In general, the system presented in (11) can hardly admit a closed-form solution since it is a linear time-varying system (unless $(1 + \dot{T})/T$ is a constant, which we will discuss in the sequel). If a quadrotor is used as the carrier, then the lack of closed-form solutions makes it challenging to implement the throw maneuver directly. A quadrotor holds the differential-flatness property, which allows to analytically derive the translational and rotational states required for performing the maneuver from the positional trajectory and its derivatives [13] (up to fourth order) and subsequently incorporated into differential-flatness-based planning [13], [14] and control [15], [16]. In practice, one can still obtain numerical values of these higher-order derivatives (e.g., acceleration, jerk, and snap) by differentiating (11). This process, however, also requires higher-order derivatives of T (i.e., $\ddot{T}$ or $\dddot{T}$), which in turn requires the higher-order derivatives of the vertical motion such as $\ddot{\boldsymbol{v}}_z$. To handle this complexity, autodifferentiation tools (e.g., CasADi [17]) can be applied to compute the required higher-order derivatives.

B. Throw maneuver with predefined landing time

In this case, we start by defining the landing time and then determine the vertical motion. This procedure results in the entire throw maneuver being governed by a set of ODEs. We first rewrite (7) into the following form:

$$\dot{\boldsymbol{v}}_z = \frac{\dot{T}g\sqrt{\boldsymbol{v}_z^2 + 2g\boldsymbol{p}_z} - g\boldsymbol{v}_z}{\sqrt{\boldsymbol{v}_z^2 + 2g\boldsymbol{p}_z} + \boldsymbol{v}_z}. \tag{12}$$

Although (12) governs the vertical motion, one can, at best, obtain numerical solutions, where computing the higher-order derivatives (e.g., those needed for the differential-flatness property of a quadrotor carrier) faces the same challenge as noted in Remark 3. Next, we will highlight two special cases, where the throw maneuver admits analytical solutions.

a) $\dot{T} = 0$*:* The landing time $T(t)$ is now a constant, i.e., $T(t) = T(0)$ for all $t \geq 0$. An immediate consequence of this choice is that (12) reduces to

$$\dot{\boldsymbol{v}}_z(t) = -\frac{1}{T(0)}\boldsymbol{v}_z(t), \tag{13}$$

which is a linear time-invariant (LTI) system that admits an analytical solution

$$\boldsymbol{v}_z(t) = \exp(-\frac{1}{T(0)}t)\boldsymbol{v}_z(0). \tag{14}$$

Furthermore, the horizontal motion becomes an LTI

$$\frac{\mathrm{d}}{\mathrm{d}t}\begin{bmatrix}\boldsymbol{p}_x \\ \boldsymbol{v}_x\end{bmatrix} = \begin{bmatrix}0 & 1 \\ 0 & -\frac{1}{T(0)}\end{bmatrix}\begin{bmatrix}\boldsymbol{p}_x \\ \boldsymbol{v}_x\end{bmatrix}, \tag{15}$$

which admits an analytical solution

$$\boldsymbol{v}_x(t) = \exp(-\frac{1}{T(0)}t)\boldsymbol{v}_x(0). \tag{16}$$

The throw maneuver, presented as closed-form solutions (14) and (16), allows one to use differential-flatness-based planners and controllers in the case of a quadrotor carrier. Furthermore, the throw maneuver admits a stationary landing time because $\dot{T} = 0$. In other words, when the carrier is on the throw maneuver, if multiple objects are released at different time instances, then the objects will *all* hit the target with the *same* duration of projectile flight.

b) $\dot{T} = -1$*:* Plugging $\dot{T} = -1$ back to (12), we know

$$\dot{\boldsymbol{v}}_z = -g. \tag{17}$$

Combining (17) with the kinematics $\dot{\boldsymbol{p}}_z = \boldsymbol{v}_z$ leads to equations of motion of a free-fall projectile with initial condition $(\boldsymbol{p}_z(0), \boldsymbol{v}_z(0))$. In other words, the carrier itself follows a projectile trajectory that leads to the target. The associated free fall of the objects is characterized by a linearly decreasing landing time, $T(t) = T(0) - t$, consistent with $\dot{T}(t) = -1$. Meanwhile, the horizontal motion proceeds with a constant velocity $\boldsymbol{v}_x(0)$.

IV. Simulation results

In this section, we numerically show throw maneuver's invariant target-hit property and compare it with a strong baseline throw method: tube acceleration [11].

A. Validating throw maneuver's invariant target-hit property

The throw maneuvers are derived with predefined vertical motions (Section III-A). Specifically, we showcase the following three vertical motions: $\boldsymbol{p}_z(t) = 10 + 0.2t^2$, $\boldsymbol{p}_z(t) = 10 - 0.2t^2$, $\boldsymbol{p}_z(t) = 10 + \sin(2\pi t/10)$. The horizontal motions are solved from (10) and (11) using the predefined vertical motions. Each maneuver in this case lasts for 5 s. In Fig. 2, we show the throw maneuver trajectories and the projectiles of objects thrown from each maneuver every second. One can see that all the projectiles hit the target, validating throw maneuver's invariant target-hit property.

B. Comparison with tube-acceleration baseline

We compare the throw maneuver with a baseline throw trajectory generation method: tube acceleration [11]. This method was originally proposed for robust manipulator-based throw against release delays within a *short* time window of length S. Here, in light of the quadrotor-based throw experiment in the next section, we simplify the tube acceleration formulation by removing the manipulator joint constrains and reducing the coordinate frame to the 2D xz-plane used in this paper, essentially keeping constraints (1b), (1c), and (1j) in [11, Problem RTV]. Consequently, we cast tube-acceleration formulation in the following form:

$$\begin{aligned}
&\text{find} && \boldsymbol{a}(\cdot) \\
&\text{subject to} && \dot{\boldsymbol{p}}(t) = \int_0^t \boldsymbol{v}(\tau)\mathrm{d}\tau + \boldsymbol{p}(0),\ \tau \in [0, S], \\
&&& \dot{\boldsymbol{v}}(t) = \int_0^t \boldsymbol{a}(\tau)\mathrm{d}\tau + \boldsymbol{v}(0),\ \tau \in [0, S], \\
&&& \Phi_{\text{fly}}(\boldsymbol{p}_x(t), \boldsymbol{p}_z(t), \boldsymbol{v}_x(t), \boldsymbol{v}_z(t)) = 0,\ \forall t \in [0, S],
\end{aligned} \tag{P$_{\text{TA}}$}$$

where $\Phi_{\text{fly}}(\cdot)$ is the flowmap that determines the horizontal landing position of an object thrown with initial position $\boldsymbol{p}$

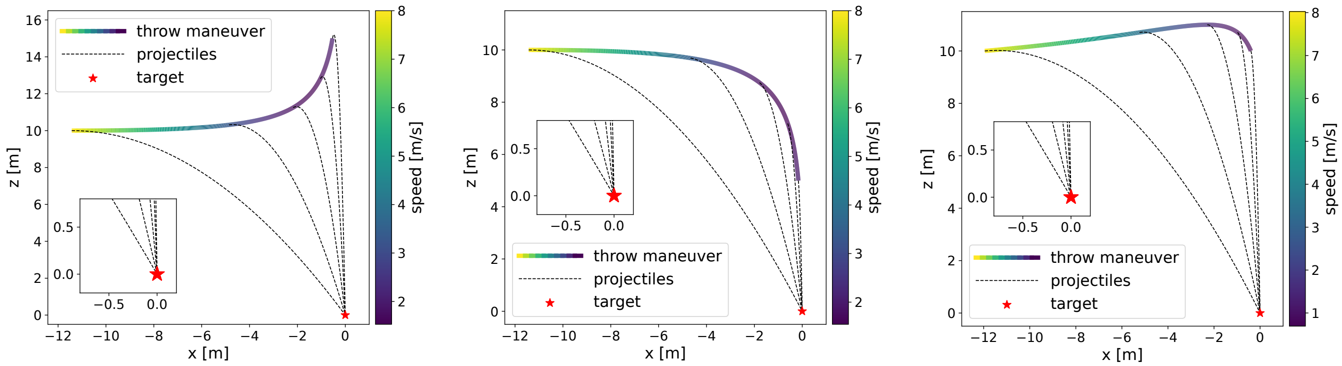

(a) $\boldsymbol{p}_z(t) = 10 + 0.2t^2$ (b) $\boldsymbol{p}_z(t) = 10 - 0.2t^2$ (c) $\boldsymbol{p}_z(t) = 10 + \sin(2\pi t/10)$

Fig. 2: Throw maneuver with predefined vertical motions shown in the sub-captions.

and initial velocity $\boldsymbol{v}$, i.e.,

$$\Phi_{\text{fly}}(\boldsymbol{p}_x, \boldsymbol{p}_z, \boldsymbol{v}_x, \boldsymbol{v}_z) = \boldsymbol{p}_x + \boldsymbol{v}_x \frac{\boldsymbol{v}_z + \sqrt{\boldsymbol{v}_z^2 + 2g\boldsymbol{p}_z}}{g}. \quad (18)$$

We use the approximation method described in [11, Section V], which leverages the short horizon S to turn (P_{TA}) to a parameter optimization problem and approximates the flowmap via its first-order approximation, i.e., the retraction constraint in [11]. As a result, tube acceleration solves the following approximation for a constant acceleration $\bar{\boldsymbol{a}}$:

$$\begin{aligned} \text{find} \quad & \bar{\boldsymbol{a}} \\ \text{s.t.} \quad & \boldsymbol{p}(S) = \boldsymbol{p}(0) + \boldsymbol{v}(0)S, \\ & \boldsymbol{v}(S) = \boldsymbol{v}(0) + \bar{\boldsymbol{a}}S, \\ & \begin{bmatrix} \frac{\partial \Phi_{\text{fly}}(0)}{\partial \boldsymbol{v}_x(0)} & \frac{\partial \Phi_{\text{fly}}(0)}{\partial \boldsymbol{v}_z(0)} \end{bmatrix} \cdot \begin{bmatrix} \boldsymbol{v}_x(S) - \boldsymbol{v}_x(0) \\ \boldsymbol{v}_z(S) - \boldsymbol{v}_z(0) \end{bmatrix} = -\Phi_{\text{fly}}(0), \end{aligned} \quad (\text{P}_{\text{TA-A}})$$

where $(\boldsymbol{p}(0), \boldsymbol{v}(0))$ belongs to the throw set $\mathcal{G}$ and

$$\Phi_{\text{fly}}(0) := \Phi_{\text{fly}}(\boldsymbol{p}_x(0) + \boldsymbol{v}_x(0)S, \boldsymbol{p}_z + \boldsymbol{v}_z(0)S, \boldsymbol{v}_x(0), \boldsymbol{v}_z(0))$$

is the target-hit offset when the object is released with delay S after the carrier passed location $\boldsymbol{p}(0)$ along a constant-velocity throw trajectory with velocity $\boldsymbol{v}(0)$.

To solve problem ($\text{P}_{\text{TA-A}}$), it suffices to solve the system equations formed by the last two equality constraints in ($\text{P}_{\text{TA-A}}$). However, there are four variables and three equations, resulting in an underdetermined system. Hence, we set zero acceleration on the vertical motion (i.e., $\bar{\boldsymbol{a}}_z = 0$) and solve for the horizontal acceleration $\bar{\boldsymbol{a}}_x$, which generates the tube-acceleration throw trajectory for comparison below. We set the initial state as $\boldsymbol{p}_x(0) = -12.1$ m, $\boldsymbol{p}_z(0) = 20$ m, $\boldsymbol{v}_x(0) = 6$ m/s, $\boldsymbol{v}_z(0) = 0$ m/s, and use throw window length of $S = 0.1$ s (same as in [11]).

For the throw maneuver, we use the derivation in Section III-B (with $\dot{T} = 0$) in this case and set the initial position and velocity as $\boldsymbol{p}(0)$ and $\boldsymbol{v}(0)$, same to those used by tube acceleration. The duration is set to 10 s for the throw maneuver.

The throw trajectories and objects' projectiles are shown in Fig. 3. First, the tube acceleration has a limited time and range to perform the throw due to the assumption on a *small* throw window S. Contrarily, the throw maneuver

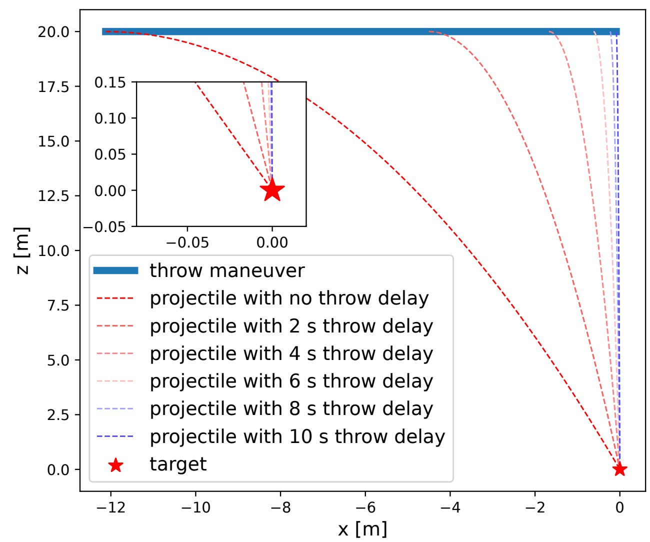

(a) Throw maneuver (proposed)

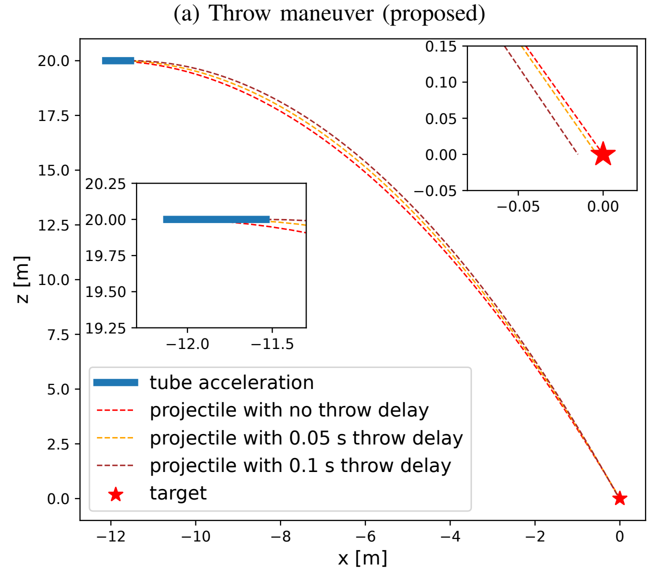

(b) Tube acceleration (baseline)

Fig. 3: Throw trajectories and projectiles of objects thrown with increasing time delays by throw maneuver and baseline tube acceleration [11]. The delay time is evenly distributed along each individual throw trajectory.

can yield arbitrarily long duration and thus has a long effective throw window (100x longer than that of the tube acceleration in this case) to throw objects. This feature is particularly useful in scenarios where multiple objects are to be sequentially thrown from a carrier, where target-hit is guaranteed with the throw maneuver regardless of the throw time. Second, the tube acceleration shows an increasing target offset when the delay on throw time increases, as seen in the enlarged detail in Fig. 3b. This phenomenon has also been mentioned in [11], which is a consequence of the first-order approximation to the flowmap. However, throw maneuver is derived in its exact form—without relaxation or approximation—and hence can theoretically guarantee no target miss, as shown in the enlarged detail in Fig. 3a and Fig. 2.

V. Experimental Results

We conduct throw experiments using a quadrotor-carrier to evaluate the accuracy and precision of the target hitting under nonideal, realistic conditions such as localization error, disturbance in control, and hardware uncertainties such as release delays. A variety of throw types are tested to represent different throw applications.

We use a custom-built quadrotor to throw golf balls to a target on the ground. The quadrotor uses 9-inch propellers and a Pixhawk flight controller. To improve the localization accuracy of outdoor flights, the quadrotor uses RTK GPS for horizontal position and a downward facing single-line lidar for height. We use the offboard flight mode in PX4 firmware to track the trajectories for throw. We program a geometric controller [15] in ROS2 that sends angular rate and thrust commands to the low-level controller in PX4 at 100 Hz. We use L1Quad [18], [19] to improve the flight robustness subject to the quadrotor's varying payload. The ROS2 system is hosted on an NVIDIA Jetson Xavier NX onboard computer running an Ubuntu 20 operating system. We install three types of throwing devices on the quadrotor as shown in Fig. 4. These devices facilitate the following throw capabilities:

1) Single throw by the soft gripper (Fig. 4A): one golf ball is thrown instantaneously upon the gripper's opening.
2) Batch throw by the lock-release magazine (Fig. 4B): multiple golf balls are thrown instantaneously upon the magazine's opening.
3) Sequential throw by the dual hopper (Fig. 4C): multiple golf balls are sequentially thrown for a period of time.

We design three experiments using these three throw devices and compare the deviation and concentration of the golf balls thrown from the throw maneuver and baseline methods in the sequel. The results are assessed by two metrics: 1. landing points' mean error to the target, which serves as a measure of target-hit accuracy; 2. circular error probable (CEP), which characterizes target-hit precision. Furthermore, we report the CEP90, defined as the radius of the circle encompassing 90% of the landing points, to quantify the spatial concentration of the impacts.

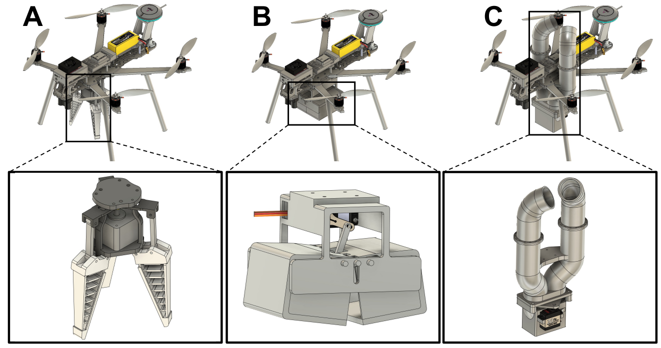

Fig. 4: CAD view of the quadrotor with different throwing devices. A: Three-fingered soft gripper with maximum load of one golf ball; B: Servo crank-slider lock-release magazine with maximum load of five golf balls; C: Dual hopper with a servo-driven rotary sector gate with maximum load of fourteen golf balls.

A. Single throw

In this experiment, we use the soft gripper (Fig. 4A) as the throw device, which has an opening delay of 0.03 s. All the throwing trajectories in this experiment are set to a constant height subject to different horizontal motions. For the throw maneuvers, we use initial height $\boldsymbol{p}_z(0)$ and horizontal velocity $\boldsymbol{v}_x(0)$ pairs of (10,6), (15,6), (20,6), (15,4), (15,8), with unit of [m, m/s]. The gripper is commanded to release the golf ball one second after the quadrotor enters the throw maneuver. We let the quadrotor throw the golf ball 10 times in each of the above height-velocity configurations. To validate that the golf ball reaches the target regardless of the throw time, we take 10 throws where we set the throw trigger time from 1 to 5.5 s (with increment of 0.5 s) after the quadrotor enters the throw maneuver. This group is referred to as the "variable throw time" (VTT) and uses the height-velocity pair of (20, 6). For baseline throw, we use hover, constant velocity, and the tube acceleration [11]. The baseline trajectories all have constant height of 20 m, where the constant velocity and tube acceleration both have (initial) horizontal velocity of 6 m/s. The tube acceleration has the same throw window $S = 0.1$ s as in simulation, which covers the opening delay of the soft gripper. The golf ball is thrown 10 times under each baseline throw.

The golf balls' landing points and confidence ellipses in this experiment are shown in Fig. 5. The landing points scatter around the target due to localization error, controller's tracking error, unmodelled interactions between the golf ball and gripper upon throwing, and mild wind. For quantitative results, we show the mean error and CEP90 in Table I. Comparing the results from the three groups of throw maneuver with 15-meter height, the landing points' mean error is more influenced by speed than by height. Specifically, a higher speed induces a bigger mean error, which is consistent with the conclusion from a sensitivity analysis to the projectile motion. The CEP90 values do not show clear dependence on height or speed, which is anticipated from the throw maneu-

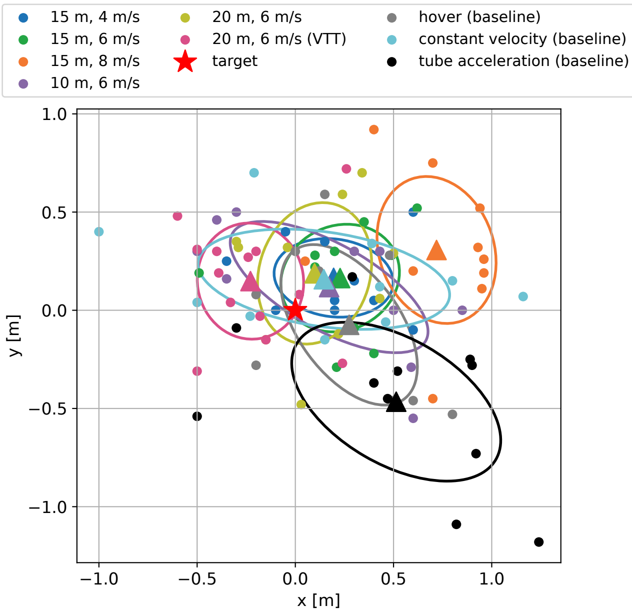

Fig. 5: Golf ball landing points in the single-throw experiment. Each ▲ marks the center location of the landing points in each group while the ellipses show the 1-sigma confidence ellipse.

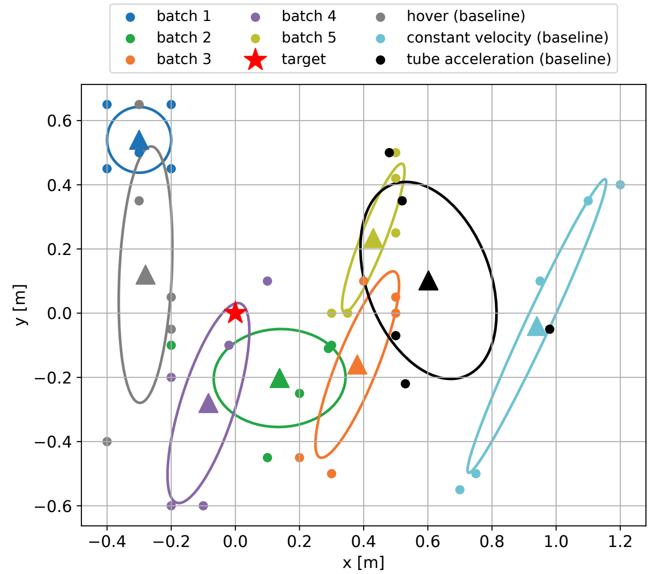

Fig. 6: Golf ball landing points in the batch-throw experiment. Each ▲ marks the center location of the landing points in each group while the ellipses show the 1-sigma confidence ellipse.

TABLE I: Statistics of landing-point distribution under single throw

Type of throw		Mean Error [m]	CEP90 [m]
Throw maneuver (proposed)	10 m, 6 m/s	0.59	0.70
	15 m, 4 m/s	**0.38**	**0.53**
	15 m, 6 m/s	0.45	**0.53**
	15 m, 8 m/s	0.87	0.69
	20 m, 6 m/s	0.46	0.57
	20 m, 6 m/s (VTT)	0.43	0.68
Hover (baseline)		0.53	0.68
Constant velocity (baseline)		0.62	1.02
Tube acceleration [11] (baseline)		0.85	0.90

TABLE II: Statistics of landing-point distribution under batch throw

Type of throw		Mean Error [m]	CEP90 [m]
Throw maneuver (proposed)	Batch 1	0.62	**0.15**
	Batch 2	**0.33**	0.25
	Batch 3	0.50	0.34
	Batch 4	0.35	0.34
	Batch 5	0.51	0.27
Hover (baseline)		0.43	0.53
Constant velocity (baseline)		1.03	0.51
Tube Acceleration (baseline)		0.68	0.41

ver's invariant target-hit property. One can also conclude that throw maneuver's target-hit is not dependent on the throw time as the mean error and CEP90 of the throwing with VTT is similar to the fixed-time throw with other height-velocity configurations. Throw maneuver's mean error and CEP90 are similar to the hover throw, because both throw trajectories hold the invariant target-hit property and hence yield similar accuracy and precision. Throw maneuver achieves smaller mean error and CEP90 than i) the constant-velocity throw, which is sensitive to the time and position of the throw action; ii) the tube-acceleration throw, which holds invariant target-hit property only under first-order approximation and can still yield target miss when the throw time is not precisely the designated time.

B. Batch throw

In this experiment, we use the lock-release magazine (Fig. 4B) as the throw device, which has an opening delay of 0.03 s. All the throwing trajectories in this experiment are set to a constant height subject to different horizontal motions. For the throw maneuvers, we use initial height $\boldsymbol{p}_z(0)$ of 20 m and horizontal velocity $\boldsymbol{v}_x(0)$ of 6 m/s. The device is commanded to release five golf balls one second after the quadrotor enters the throw maneuver. We let the quadrotor repeat the throw five times. The baseline throws include hover, constant velocity, and tube acceleration, where the height-velocity configurations are identical to that of the single throw.

The golf balls' landing points and confidence ellipses in this experiment are shown in Fig. 6. The ellipses are mostly stretched because the lock-release magazine exerts small initial speed to the golf balls along the y-axis when open to throw balls. The mean error and CEP90 are reported in Table II, where the throw maneuver's target-hit accuracy and precision are close to those by hover throw and better than the constant-velocity throw and tube-acceleration throw for reasons analyzed in Section V-A. The batch throw has better concentration than the repeated single throws (as indicated by the CEP90 values) because the former has one throw location in each throw whereas the latter's repeated throws

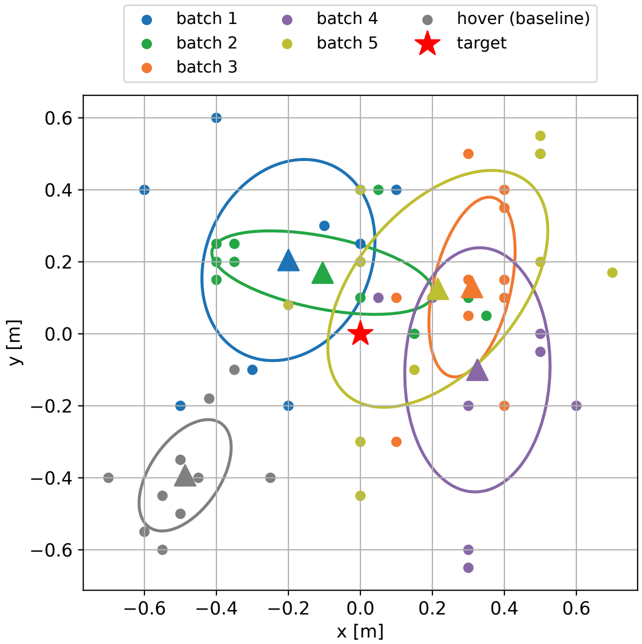

Fig. 7: Golf ball landing points in the sequential-throw experiment. Each ▲ marks the center location of the landing points in each group while the ellipses show the 1-sigma confidence ellipse.

have distinctive throw locations subject to localization and control errors.

C. Sequential throw

In this experiment, we use the dual hopper (Fig. 4C) as the throw device. All the throwing trajectories in this experiment are set to a constant height subject to different horizontal motions. For the throw maneuvers, we use initial height $\boldsymbol{p}_z(0)$ of 20 m and horizontal velocity $\boldsymbol{v}_x(0)$ of 6 m/s. The device is commanded to throw 10 golf balls sequentially within 1.33 s after one second when the quadrotor enters the throw maneuver. We let the quadrotor repeat the throw five times. We only use hover throw as the baseline in this experiment because of its invariant target-hit property. The constant-velocity and tube acceleration are not used: the former yields enormously stretched distribution of landing points, whereas the 1.33-second duration of throw window violates the latter's assumption on short time throw interval. The projectiles of the golf balls in this experiment are shown in the long exposure Fig. 1D.

The golf balls' landing points and confidence ellipses in this experiment are shown in Fig. 7. Landing points by the throw maneuver are closer to the target than the baseline hover throw, which is also indicated by the mean errors in Table III. This might be caused by the GPS's localization error when performing the hover throw. Nevertheless, the concentration by throw maneuver is slightly inferior to that of the hover throw, most likely due to the quadrotor's imperfect trajectory tracking.

TABLE III: Statistics of landing-point distribution under sequential throw

Type of throw		Mean Error [m]	CEP90 [m]
Throw maneuver (proposed)	Batch 1	0.42	0.44
	Batch 2	**0.35**	0.41
	Batch 3	0.41	0.37
	Batch 4	0.44	0.55
	Batch 5	0.45	0.51
Hover (baseline)		0.64	**0.24**

D. Discussion

With different throw devices, we show that the throw maneuver's landing points have better accuracy and precision than constant-velocity throw and the tube-acceleration throw and have achieved similar performance to the naive baseline of hover throw. While the hover throw is appealing for its simplicity in implementation, throw maneuver is a kinetic throw that holds the invariant target-hit property as hover throw does. The kinetic feature of throw maneuver provides advantages over hover throw in time-critical applications such as wild land firefighting.

Consider using a heavy lift multirotor vehicle carrying a water tank to quickly put out spot fire before it develops to larger, uncontrollable fire. A simple solution is to have the multirotor vehicle approach a location on top of the fire, hover for a period of time to kill the kinetic energy of the slosh water in the tank, only then to drop the water over the fire in a steady position hold. This procedure is time-consuming because it requires to deaccelerate to a full stop and establish a steady position hold to effectively drop the water to the fire. If the vehicle performs the throw maneuver, the water drop can be triggered without needing to come to a full stop and the water can still land on the fire. The time and fuel efficiency of water drops using the throw maneuver surpass those of the hover throw in collaborative firefighting scenarios. With the throw maneuver, multiple aerial vehicles can release water sequentially in non-stop flights, maximizing the total water volume delivered per unit time. In contrast, hover throw is constrained by the inevitable delays required to stop and hold position.

Despite the advantageous features of the throw maneuver, several limitations remain. Achieving high target-hitting accuracy requires the carrier to closely follow the prescribed throw trajectory, which imposes stringent demands on localization accuracy and control performance. Moreover, the current formulation neglects aerodynamic drag, which can dominate in certain throwing applications. Incorporating drag into the derivation of the throw maneuver would preclude analytical solutions and necessitate numerical methods.

VI. Conclusion

We propose throw maneuver: a carrier trajectory that yields invariant target-hit for objects thrown from the carrier at any moment. By differentiating the governing projectile equations, we derive the ODEs that exactly characterize the throw maneuver. Simulation results confirm its the invariant target-hit property and demonstrate its advantages over the baseline tube-acceleration throw in terms of much longer time window and range to throw as well as no target miss. Outdoor quadrotor experiments further validate the approach, showing improved accuracy and precision compared with kinetic baseline throw methods in realistic conditions.

Future work will extend the framework to account for aerodynamic drag effects on the thrown object and to enhance localization and control accuracy, thereby further improving the reliability and precision of robotic throwing in practical settings.

Acknowledgment

The authors would like to thank Yixiao Liu for capturing the long-exposure photo.

References

[1] T. Senoo, A. Namiki, and M. Ishikawa, "High-speed throwing motion based on kinetic chain approach," in *Proceedings of IEEE/RSJ International Conference on Intelligent Robots and Systems*. IEEE, 2008, pp. 3206–3211.

[2] Y. Zhang, J. Luo, and K. Hauser, "Sampling-based motion planning with dynamic intermediate state objectives: Application to throwing," in *Proceedings of IEEE International Conference on Robotics and Automation*. IEEE, 2012, pp. 2551–2556.

[3] A. Sintov and A. Shapiro, "A stochastic dynamic motion planning algorithm for object-throwing," in *Proceedings of IEEE International Conference on Robotics and Automation*. IEEE, 2015, pp. 2475–2480.

[4] F. Lombai and G. Szederkényi, "Throwing motion generation using nonlinear optimization on a 6-degree-of-freedom robot manipulator," in *Proceedings of IEEE International Conference on Mechatronics*. IEEE, 2009, pp. 1–6.

[5] Z. Li, H. Chen, Y. Lin, B. Ye, and X. Lyu, "AeroThrow: An autonomous aerial throwing system for precise payload delivery," *arXiv preprint arXiv:2507.13903*, 2025.

[6] W. Mori, J. Ueda, and T. Ogasawara, "1-dof dynamic pitching robot that independently controls velocity, angular velocity, and direction of a ball: Contact models and motion planning," in *Proceedings of IEEE International Conference on Robotics and Automation*. IEEE, 2009, pp. 1655–1661.

[7] H. Miyashita, T. Yamawaki, and M. Yashima, "Control for throwing manipulation by one joint robot," in *Proceedings of IEEE International Conference on Robotics and Automation*. IEEE, 2009, pp. 1273–1278.

[8] L. Werner, F. Nan, P. Eyschen, F. A. Spinelli, H. Yang, and M. Hutter, "Dynamic throwing with robotic material handling machines," in *Proceedings of IEEE/RSJ International Conference on Intelligent Robots and Systems*. IEEE, 2024, pp. 98–104.

[9] A. Zeng, S. Song, J. Lee, A. Rodriguez, and T. Funkhouser, "TossingBot: Learning to throw arbitrary objects with residual physics," 2019.

[10] A. Pekarovskiy and M. Buss, "Optimal control goal manifolds for planar nonprehensile throwing," in *Proceedings of IEEE/RSJ International Conference on Intelligent Robots and Systems*. IEEE, 2013, pp. 4518–4524.

[11] Y. Liu and A. Billard, "Tube acceleration: robust dexterous throwing against release uncertainty," *IEEE Transactions on Robotics*, vol. 40, pp. 2831–2849, 2024.

[12] Y. Ma, Y. Liu, K. Qu, and M. Hutter, "Learning accurate whole-body throwing with high-frequency residual policy and pullback tube acceleration," *arXiv preprint arXiv:2506.16986*, 2025.

[13] D. Mellinger and V. Kumar, "Minimum snap trajectory generation and control for quadrotors," in *Proceedings of IEEE International Conference on Robotics and Automation*. IEEE, 2011, pp. 2520–2525.

[14] Z. Wang, X. Zhou, C. Xu, and F. Gao, "Geometrically constrained trajectory optimization for multicopters," *IEEE Transactions on Robotics*, vol. 38, no. 5, pp. 3259–3278, 2022.

[15] T. Lee, M. Leok, and N. H. McClamroch, "Geometric tracking control of a quadrotor UAV on SE(3)," in *Proceedings of the 49th IEEE Conference on Decision and Control*, Atlanta, GA, USA, 2010, pp. 5420–5425.

[16] S. Sun, A. Romero, P. Foehn, E. Kaufmann, and D. Scaramuzza, "A comparative study of nonlinear mpc and differential-flatness-based control for quadrotor agile flight," *IEEE Transactions on Robotics*, vol. 38, no. 6, pp. 3357–3373, 2022.

[17] J. A. E. Andersson, J. Gillis, G. Horn, J. B. Rawlings, and M. Diehl, "CasADi – A software framework for nonlinear optimization and optimal control," *Mathematical Programming Computation*, vol. 11, no. 1, pp. 1–36, 2019.

[18] Z. Wu, S. Cheng, K. A. Ackerman, A. Gahlawat, A. Lakshmanan, P. Zhao, and N. Hovakimyan, "L1 adaptive augmentation for geometric tracking control of quadrotors," in *Proceedings of 2022 International Conference on Robotics and Automation*. IEEE, 2022, pp. 1329–1336.

[19] Z. Wu, S. Cheng, P. Zhao, A. Gahlawat, K. A. Ackerman, A. Lakshmanan, C. Yang, J. Yu, and N. Hovakimyan, "L1Quad: L1 adaptive augmentation of geometric control for agile quadrotors with performance guarantees," *IEEE Transactions on Control Systems Technology*, vol. 33, no. 2, pp. 597–612, 2025.